

# Scaling invariance of the diffusion coefficient in a family of two-dimensional Hamiltonian mappings

Juliano A. de Oliveira<sup>1</sup>, Carl P. Dettmann<sup>2</sup>, Diogo R. da Costa<sup>3</sup> and Edson D. Leonel<sup>1,4</sup>

<sup>1</sup> *Departamento de Estatística, Matemática Aplicada e Computação - UNESP - Univ Estadual Paulista, Av.24A, 1515 - 13506-900 - Rio Claro - SP - Brazil*

<sup>2</sup> *School of Mathematics, University of Bristol, Bristol BS8 1TW, United Kingdom*

<sup>3</sup> *Instituto de Física da USP, Rua do Matão, Travessa R, 187 - Cidade Universitária - 05314-970 - São Paulo - SP - Brazil*

<sup>4</sup> *Departamento de Física - UNESP - Univ Estadual Paulista, Av.24A, 1515 - 13506-900 - Rio Claro - SP - Brazil*

(Dated: October 22, 2012)

We consider a family of two-dimensional nonlinear area preserving mappings that generalize the Chirikov standard map and model a variety of periodically forced systems. The action variable diffuses with increments whose phase is controlled by a negative power of the action and hence effectively uncorrelated for small actions, leading to a chaotic sea in phase space. For larger values of the action the phase space is mixed and contains a family of elliptic islands centered on periodic orbits and invariant KAM curves. The transport of particles along the phase space is considered by starting an ensemble of particles with a very low action and letting them evolve in the phase until they reach a certain height  $h$ . For chaotic orbits below the periodic islands, the survival probability for the particles to reach  $h$  is characterized by an exponential function, well modelled by the solution of the diffusion equation. On the other hand when  $h$  reaches the position of periodic islands, the diffusion slows markedly. We show that the diffusion coefficient is scaling invariant with respect to the control parameter of the mapping when  $h$  reaches the position of the lowest KAM island.

PACS numbers: 05.45.-a, 05.45.Pq, 05.45.Tp

Characterizing mixed regular-chaotic phase space remains one of the most challenging open problems in Hamiltonian dynamics. When there is periodic forcing, the level of chaoticity is typically controlled by the ratio of the intrinsic and extrinsic timescales, a function of phase space variables. For example, the family of maps

$$T : \begin{cases} J_{n+1} = |J_n - \epsilon \sin(2\pi\theta_n)| \\ \theta_{n+1} = [\theta_n + J_{n+1}^{-\gamma}] \pmod{1} \end{cases}, \quad (1)$$

for action  $J$  and angle  $\theta$  describe a large class of systems, including for  $\gamma = 3/2$  the diffusion of the orbital parameters of comets due to the periodic motion of Jupiter [1, 2] or dynamics in a wave packet [3], for  $\gamma = 1$  a particle moving between a vibrating and a fixed plate [4] and periodically corrugated waveguide [5], for  $\gamma = 1/2$  a time-dependent potential well [6, 7], for  $\gamma = 2$  it may be relevant for plasma physics [8], while for  $\gamma = -1$  a particle bouncing on a vibrating plate [9] and closely related Chirikov standard map [10]. For clarity we will henceforth assume that  $\gamma > 0$ , although the case  $\gamma < 0$  can be treated similarly. The time scale separation is given by  $J^{-\gamma}$  so that when  $J \approx 1$  there is mixed phase space, while  $J \ll 1$ ,  $\theta$  is effectively random, leading to strongly chaotic diffusion of  $J$  which can be described analytically. Here we develop an open systems approach as a sensitive probe of both chaotic and mixed regions, and demonstrate scale invariance of the diffusion coefficient with respect to the control parameter  $\epsilon$ .

A powerful technique for analysing dynamical systems [11, 12] involves placing an absorbing “hole” when  $J > h$  for some hole parameter  $h$  while specifying the distribution of initial conditions, hence defining the (“survival”)

probability  $P(n)$  that the action will remain less than  $h$  until  $n$  collisions. This provides a sensitive test of the diffusion of the action variable. In the strongly chaotic regime,  $P(n) \sim e^{-An}$  with an escape rate  $A$  that can be predicted by solving the diffusion equation with appropriate initial and boundary conditions and without any free parameters. Relation of transport (for example diffusion) coefficients to the escape rate  $A$  in molecular systems was introduced as “the escape rate formalism” [13, 14]. Here the diffusion is in phase space, and furthermore we predict the full time dependence  $P(n)$ .

As the action rises, periodic motion is observed leading to the existence of Kolmogorov-Arnold-Moser (KAM) islands. For even higher values of the action a set of invariant KAM curves (also called as invariant spanning curves or rotational invariant circles) is present in the phase space limiting the unbounded growth of the action. Due to the existence of periodic islands, the orbits may spend a time trapped around the regular regions. This temporary trapping, also known as stickiness, affects directly the diffusion coefficient, which markedly changes at the position of the periodic island. Thus the relevant scale for the onset of stickiness is the location of the lowest stable island  $J_{LSI}$ . In this Letter we show that the sticky diffusion process is scale invariant, in that the scaled diffusion coefficient  $D/\epsilon^2$  calculated using the open systems approach is an universal function of the scaled hole height  $h/J_{LSI}$ .

We now consider the dynamics in the chaotic sea, that is, for small values of  $J$ . Due to the lack of correlations of the angle variable, the increments in  $J$  are well described using a central limit theorem (CLT) [15, 16], so that

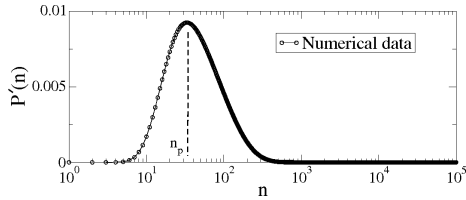


FIG. 1: (Colour online) Plot of  $P'$  vs.  $n$  considering  $h = 10$  and  $D = 0.5$ .

over many time steps, the distribution of displacements is Gaussian with a variance exactly proportional to the number of steps. Sufficient conditions for a CLT to hold are that  $\{X_n\}_{n=1}^{\infty}$  is a sequence of Independent and Identically Distributed (IID) real valued random variables such that: (i) the mean  $\langle X_n \rangle = 0$  and; (ii)  $\langle X_n^2 \rangle < \infty$  [17–19]. In Eq. (1) we see that the angles diverge in the limit of vanishing action and are thus expected to be independent and uniformly distributed on  $[0, 1)$ . The increment of  $J$  in Eq. (1) and also in many physical problems in the literature [20] is given by  $\Delta_n = J_{n+1} - J_n = -\epsilon \sin(2\pi\theta_n)$ , and is also IID. Then, it is possible to observe that  $\langle \Delta_n^2 \rangle = \int_0^1 \epsilon^2 \sin^2(2\pi\theta) d\theta = \epsilon^2/2$ . Therefore the analytical diffusion coefficient is given by  $D = \langle \Delta^2 \rangle / 2 = \epsilon^2/4$ , and hence  $D/\epsilon^2 = 1/4$ . We have ignored the absolute value signs here for  $J < \epsilon$ ; their effect is to ensure that  $J$  remains positive, that is, there is a rigid wall in the diffusion process at  $J = 0$ .

Over many iterations, we may consider the continuum process given by the diffusion equation

$$\frac{\partial u}{\partial n} = D \frac{\partial^2 u}{\partial J^2}, \quad (2)$$

where  $u$  is the probability density function. The boundary conditions are given by  $du/dJ(0, n) = 0$  (the rigid wall, above) and  $u(h, n) = 0$  (escape through the hole). This problem may be solved by separation of variables,  $u(J, n) = X(J)T(n)$ , where the boundary conditions give  $X(J) = \cos[J\pi(k + 1/2)/h]$ , with  $k = 0, 1, 2, 3, \dots$ . Substituting for  $u(J)$  in Eq. (2), we obtain the solution of the diffusion equation,

$$u(J, n) = \sum_{k=0}^{\infty} a_k \cos \left[ \frac{J\pi(k + \frac{1}{2})}{h} \right] \exp \left[ \frac{-Dn\pi^2(k + \frac{1}{2})^2}{h^2} \right]. \quad (3)$$

Finally, the unknown coefficients  $a_k$  are determined by the initial conditions. Here we start all the particles near  $J = 0$ , so that  $u(J, 0) = \delta(J)$ . Equating this with  $a_k \cos[J\pi(k + 1/2)/h]$  as required for Eq. (3), multiplying both sides by  $\cos[J\pi(m + 1/2)/h]$  and integrating as a function of  $J$  over  $[0, h]$  yields

$$u(J, n) = \frac{2}{h} \sum_{k=0}^{\infty} \cos \left[ \frac{J\pi(k + \frac{1}{2})}{h} \right] \exp \left[ \frac{-Dn\pi^2(k + \frac{1}{2})^2}{h^2} \right], \quad (4)$$

which obeys Eq. (2), both boundary conditions and the initial condition. Integrating Eq. (4) as a function of  $J$

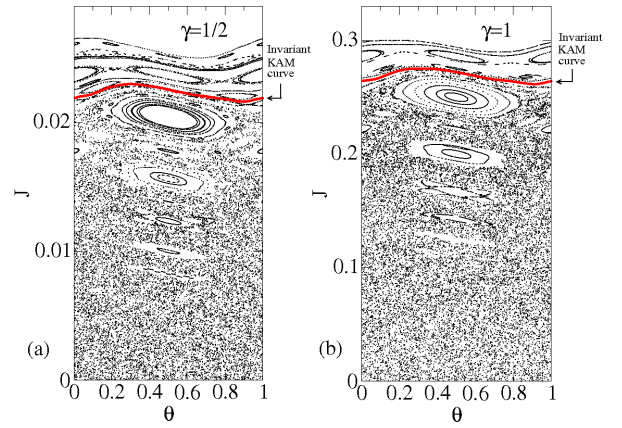


FIG. 2: (Colour online) Phase space using: (a)  $\epsilon = 10^{-3}$  and  $\gamma = 1/2$ , (b)  $\epsilon = 10^{-2}$  and  $\gamma = 1$ .

in the range of  $[0, h]$ , the survival probability is given by

$$P(n) = \frac{2}{\pi} \sum_{k=0}^{\infty} \frac{\sin \left[ \pi(k + \frac{1}{2}) \right]}{k + \frac{1}{2}} \exp \left[ \frac{-Dn\pi^2(k + \frac{1}{2})^2}{h^2} \right]. \quad (5)$$

The negative of the derivative of  $P(n)$  with respect to  $n$ , i.e.,  $P'(n) = dP(n)/dn$ , furnishes the histogram of frequency for the number of particles that escaped at a time  $n$ . A plot of  $P'(n)$  vs.  $n$  is shown in Fig. 1. We see from such figure that for short  $n$  there is a regime of growth of the histogram of frequency. It then reaches a maximum at  $n_p$  and decreases later on for large  $n$ . Few particles can travel the distance  $h$  and so escape at short times. The peak denotes the typical  $n$  where the majority of the ensemble is assumed to reach  $h$ . At late times there are few particles remaining, and so the number that escape decreases. Considering Fig. 1 together with the expression of  $P'(n)$ , we can see for high values of  $h$  that the single term  $k = 0$  dominates and so  $\exp[-Dn\pi^2/(4h^2)] \cong \exp[-An]$ . Thus the diffusion coefficient is written as

$$D = \frac{4h^2 A}{\pi^2}. \quad (6)$$

The coefficient  $A$  may be obtained by fitting an exponential on the histogram of frequency  $P'(n)$  vs.  $n$  for the decaying curve after the peak and before the final tail of the curve (which may not be exponential due to the stickiness).

The above results are very general, applying to any system modeled by the diffusion equation in this way. We now consider more specifically the family of mappings given in Eq. (1). The control parameters are  $\epsilon$  and  $\gamma$ . For  $\epsilon = 0$  the system is integrable while it is mixed for any  $\epsilon \neq 0$ . The mapping is area preserving since the determinant of the Jacobian matrix is equal to one. The relevance of particular values of  $\gamma$  is given in the introduction. The phase space generated from mapping (1) is shown in Fig. 2 for the control parameters: (a)  $\epsilon = 10^{-3}$  and  $\gamma = 1/2$

and (b)  $\epsilon = 10^{-2}$  and  $\gamma = 1$ . One sees the phase space is mixed, with strong chaos at small  $J$ , a set of KAM islands that are surrounded by a chaotic sea that is limited by a set of invariant KAM curves.

The size of the chaotic sea can be estimated using the position of the lowest invariant KAM curve. As discussed in [21], near such a curve, the action can be approximated as  $J_{n+1} \cong J^* + \Delta J_{n+1}$  where  $J^*$  is a typical value along of the curve and  $\Delta J_{n+1}$  is a small perturbation of  $J^*$ . Using this approximation and making a connection with the Chirikov standard map [10], which has a transition from local to global chaos at  $K = 0.9716\dots$ , the first invariant KAM curve can be described as  $J^* \cong \left[ \frac{2\pi\gamma\epsilon}{0.9716\dots} \right]^{1/(1+\gamma)}$ . The diffusion equation given by (2) and the diffusion coefficient obtained from Eq. (6) can be applied well for the chaotic region of the phase space generated by mapping (1) below the lowest action KAM island. When the islands of stability are considered, local trapping may be observed. This stickiness regime affects directly the transport of particles in the phase space leading to a markedly reduction of the diffusion coefficient  $D$  (as we shall see in Fig. 4). The understanding of the effects of stickiness in transport is still a major open problem.

The boundary conditions in the phase space are defined by the lowest value of the action (for instance zero) and the position  $h < J^*$  which defines the upper absorber. To average the quantities, we start with an ensemble of several different initial conditions at very low initial action as  $10^{-3}\epsilon$  and different angles  $\theta_0$  uniformly distributed along  $\theta_0 \in [0, 1]$ . If during the dynamics the particle reaches  $h$ , the simulation is stopped at that time, the number of iterations  $n$  needed for the diffusion of the particle until reaching  $h$  is collected from the dynamics and a new initial condition is started with a different angle. The process is repeated until the entire ensemble is considered. If the maximum length of time of  $n = 10^5$  allowed for the dynamics is reached, we consider that the particle has not escaped (it may escape latter and for a longer run) and a new initial condition is started.

It is known that when the escape is considered in a region where only chaos is present, the survival probability of an ensemble of particles moving in such a region is described by an exponential decay (see for instance [22, 23]). The existence of periodic regions in the phase space including islands of stability and invariant tori lead to local trapping due to stickiness [24–26] and consequently to anomalous diffusion [27] transforming the decay of the survival probability into a slower regime that may include either a power law [28, 29] or even stretched exponential [30]. In our simulations, the position  $h$  (upper boundary for escape) was varied. For values of  $h$  below the stability regions, an exponential decay describes well the survival probability while a slower decay is observed when periodic islands are present. Figure 3(a) shows a plot for the histogram of frequency (rescaled to have peak at one for visual purposes) considering the parameters  $\gamma = 3/4$  and  $\epsilon = 10^{-4}$  although any other set of control parameters generate similar plot, therefore the

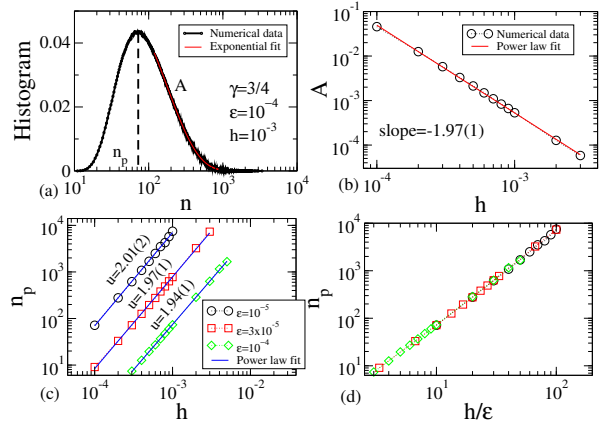


FIG. 3: (Colour online) For  $\gamma = 3/4$  we have: (a) A plot of Histogram as a function of  $n_p$ , where we highlight how to find  $n_p$ ; (b)  $A$  vs.  $h$ , where the slope is equal to  $-1.97(1)$ ; (c)  $n_p$  vs.  $h$  for different values of  $\epsilon$ :  $\epsilon = 10^{-5}$ ,  $\epsilon = 3 \times 10^{-5}$  and  $\epsilon = 10^{-4}$  and (d)  $n_p$  vs.  $h/\epsilon$ .

behavior seems to be generic for any  $\gamma > 0$  and  $\epsilon \neq 0$ . The parameter  $A$  used in Eq. (6) is obtained by a numerical fitting of the decay of the curve after reaching the peak at  $n_p$  and before the final tail (where fluctuations due to the size of the ensemble or the size of the bins have influence). Figure 3(b) shows a plot of  $A$  vs.  $h$  and a power law fitting gives the slope as  $-1.97(1) \cong -2$  in good agreement with Eq. (6). The peak of the histogram is also sensible to the position of  $h$ . It moves to the right in Fig. 3(a) when the position of  $h$  is raised in the vertical and moves to the left when  $h$  moves down in the phase space. This behavior is indeed expected because as higher  $h$ , the larger  $n$  the mapping (1) must be iterated for the particle to reach  $h$ . A plot of  $n_p$  vs.  $h$  is shown in Fig. 3(c). If the position  $h$  is rescaled as  $h \rightarrow h/\epsilon$ , the different curves of  $n_p$  obtained for different  $\epsilon$  are overlapped onto a single plot as shown in Fig. 3(d).

Let us now discuss our numerical results obtained for the diffusion coefficient. From numerical simulations, we obtained different values for the coefficient  $A$  and Eq. (6) was evaluated. The diffusion coefficient is shown in Fig. 4(a) for different control parameters  $\epsilon$  and  $\gamma$ . Different control parameter  $\epsilon$  generate different values for  $D$  in agreement with  $D/\epsilon^2 = 1/4$ . We notice that  $D$  is almost constant for a large range of  $h$  when it suddenly suffers a marked decrease. The decrease happens because the position  $h$  reached the lowest action KAM island. From fixed point stability analysis we found that the position of the last period one fixed point, generating the last period one island is located at

$$J_{LSI} \cong \left[ \frac{\gamma\pi\epsilon}{2} \right]^{\frac{1}{1+\gamma}}, \quad (7)$$

where the index  $LSI$  stands for lowest stable KAM island. We see there are two different types of scaling for the behavior of  $D$ . The first scaling is observed for very small values of  $h$ . At this region, presumably there is

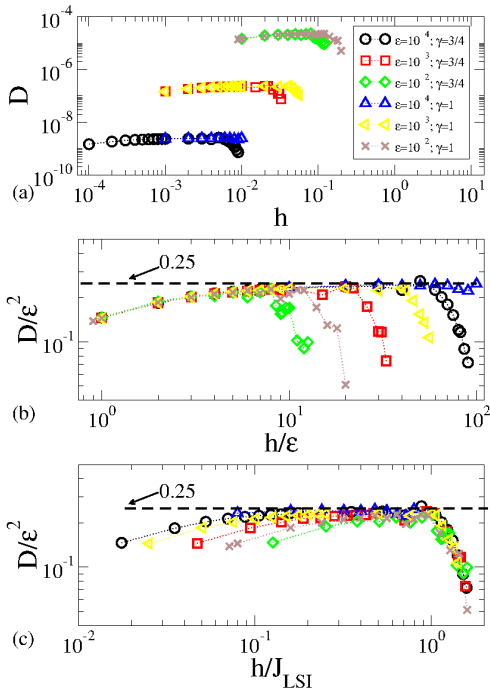


FIG. 4: (Colour online) (a)  $D$  vs.  $h$  for different values of  $\epsilon$  and  $\gamma$ . (b) After a rescaling in the axis, the curves collapsed for small values of  $h$ . (c) After a properly rescaling in the axis, all curves collapsed for high values of  $h$ .

breakdown of the continuum approximation used in the diffusion equation since  $h$  comes close enough to the scale of the variation of  $\epsilon$ . Figure 4(b) shows the behavior of

$D$  for the rescale  $D \rightarrow D/\epsilon^2$  and  $h \rightarrow h/\epsilon$ . We see clearly that all curves of  $D$  obtained for different control parameters as shown in Fig. 4(a) overlap each other for low values of  $h/\epsilon$  but differ for large  $h$ . The striking result is obtained when the horizontal axis is rescaled with respect to the position of the lowest stable KAM island as given by Eq. (7), i.e.  $h \rightarrow h/J_{LSI}$ , as shown in Fig. 4(c). In addition we see that despite the short difference of  $D/\epsilon^2$  for the different control parameter  $\epsilon$  considering short  $h$ , the diffusion coefficient suffers a sudden change when the position  $h$  reaches periodic KAM islands. Because of the periodic regions, the particles may suffer temporary trapping due to stickiness and influence on the transport along the phase space. At that point normal CLT is not observed anymore consequently the CLT is not applicable at such domain.

It would be interesting to investigate whether a modified, perhaps fractional, diffusion equation could apply to the variation of  $J$  in the sticky region, and whether the same kind of stickiness is present at the impenetrable lowest invariant spanning curve. Many of the applications, including the Kepler (now Coulomb) problem and motion in the presence of a vibrating wall, make sense in the microscopic domain, where quantum effects reign.

Acknowledgments: JAO thanks to CAPES and PROPE/UNESP. CPD and DRC are grateful to FAPESP. EDL thanks to FAPESP, CNPq and FUNDUNESP, Brazilian agencies. This research was supported by resources supplied by the Center for Scientific Computing (NCC/GridUNESP) of the São Paulo State University (UNESP).

- 
- [1] G.M. Zaslavsky, Hamiltonian chaos and fractional dynamics. Oxford University Press, Oxford, (2005).
- [2] I. I. Shevchenko, New Astron. **16**, 94(2011).
- [3] Zaslavsky G.M., Sagdeev R.D., Usikov D.A. and Chernikov A.A.: Weak Chaos and Quasi-Regular Patterns. Cambridge University Press, Cambridge (1991).
- [4] M. A. Lieberman, A. J. Lichtenberg, Phys. Rev. A **5**, 1852 (1971).
- [5] G. A. Luna-Acosta, J. A. Mendez-Bermudez, and F. M. Izrailev, Phys. Rev. E **64**, 036206 (2001); Phys. Lett. A **274**, 192 (2000).
- [6] G. A. Luna-Acosta, G. Orellana-Rivadeneira, A. Mendoza-Galván, and C. Jung, Chaos, Solitons and Fractals, **12**, 349 (2001).
- [7] J. L. Mateos, Phys. Lett. A, **256**, 113 (1999).
- [8] Zaslavsky G. M., Sagdeev R. D., Usikov D. A. and Chernikov A. A, *Weak Chaos and Quasi-Regular Patterns*. Cambridge University Press, Cambridge 1991.
- [9] L. D. Pustynnikov, Trans. Moscow Math. Soc. **2**, 1 (1978).
- [10] A. J. Lichtenberg, M. A. Lieberman, *Regular and chaotic dynamics* **38**, (NY: Springer Verlag) 1992.
- [11] L. A. Bunimovich and C. P. Dettmann, EPL, **80**, 40001 (2007).
- [12] E. G. Altmann, S. E. Portela and Tamas Tel, arxiv:1208.0254.
- [13] P. Gaspard and G. Nicolis, Phys. Rev. Lett. **65**, 1693(1990).
- [14] J. R. Dorfman and P. Gaspard, Phys. Rev. E **51**, 28(1995).
- [15] W. J. Adams, The Life and times of the Central Limit Theorem. 2.ed. American Mathematical Society, Providence (2009).
- [16] H. Fischer, History of the Central Limit Theorem. Springer, New York (2011).
- [17] I. Eliazar, J. Klafter, Chem. Phys. **370**, 290 (2010).
- [18] H. J. Hilhorst, Braz. J. Phys **39**, 371 (2009).
- [19] S. Umarov, C. Tsallis, S. Steinberg, Milan J. Math. **76**, 307 (2008).
- [20] G. M. Zaslavsky, Phys. Rep. **371**, 461 (2002).
- [21] E. D. Leonel, J. A. de Oliveira and F. Saif. J. Phys. A **44**, 302001 (2011).
- [22] C. F. F. Karney, Physica D **8**, 360, 1983.
- [23] M. F. Demers and L.-S. Young, Nonlinearity **19** 377 (2006).
- [24] V. A. Avetisov and S. K. Nechaev, Phys. Rev. E **81**, 046211 (2010).
- [25] D. L. Shepelyansky, Phys. Rev. E **82**, 055202(R) (2010).
- [26] G. Cristadoro, R. Ketzmerick, Phys. Rev. Lett. **100**,

- 184101 (2008).
- [27] S. S. Abdullaev and K. H. Spatschek, Phys. Rev. E **60**, R6287 (1999).
- [28] H. Henry et. al., Chaos **9**, 381 (1999).
- [29] N. Buric, A. Rampioni, G. Turchetti and S. Vaienti, J. Phys. A: Math. Gen. **36**, L209 (2003).
- [30] C. P. Dettmann and E. D. Leonel, Physica D **241**, 403 (2012).